

# Hydrodynamic Poroelasticity with Thermal Effects

Michael Eden<sup>†</sup>, Meraj Alam<sup>\*</sup>, Prakash Kumar<sup>‡</sup>, and Raja GP Sekhar<sup>§</sup>

<sup>†</sup>Karlstad University, Karlstad, Sweden

<sup>\*</sup>Mahindra University, Hyderabad, India

<sup>‡</sup>SRM University AP, Amaravati, India

<sup>§</sup>IIT Kharagpur, Kharagpur, India

February 11, 2025

This study proposes and explores a linear hydrodynamic thermo-elasticity system within the context of mixture models, encompassing fluid and solid phases, with particular emphasis on biological tissues and tumor-related phenomena. While tumor growth dynamics are not explicitly modeled yet, this work examines the interaction between thermal effects and hydrodynamics on short-time scales where the tumor size typically remains stable. We establish the existence of a unique weak solution within the framework of implicit evolution equations where we exploit the intricate coupling mechanisms inherent to the PDE system. To further investigate the model, we then study the one-dimensional model and explore in detail the complex interplay between fluid flow, solid deformation, and heat transfer. This complex coupled system of equations is then reduced over a short time scale to obtain semi-analytical solutions.

**Keywords:** Mixture theory, thermoelasticity, modeling of biological tissue, coupled PDE systems  
**MSC2020:** 74E30, 74F05, 74F10, 35M30

## 1 Introduction

Modeling the mechanical behavior of biological tumors using porous medium equations is very common [5, 31]. However, considering the elastic nature of the tumor structure, there are two commonly known approaches for modeling soft tissue, namely the theory of poroelasticity (we point to [12]) and the theory of mixture (e.g., [9]). In the former, soft tissues are supposed to exhibit sponge-like behavior as fluid-saturated elastic porous solids, whereas in the latter, the continuous binary mixture of the solid (s) and fluid (f) phases represents the dynamics. To estimate the temperature effect on solid deformations, thermal expansion effects are to be considered in the constitutive equations, and these equations are termed thermoporoelasticity theory [4]. Detailed literature review indicates that the scientific community has only recently begun showing enthusiasm to understand the effects of thermal expansion on fluid transport in tissues.

Pioneering work on mixtures as continua interacting can be assigned to Truesdell and Toupin [11] and Green and Naghdi [22, 23]. Consequently, several authors have considered the mathematical analysis involving mixtures of elastic and viscoelastic constituents. Iesan [24] developed the theory of binary mixtures of thermoelastic solids where each of the phases is treated as thermoelastic solid. The corresponding dependent variables are displacement gradients, relative displacement, temperature and temperature gradient. They have shown a uniqueness theorem for the governing system of thermoelasticity for linear theory. In [36], the authors considered diffusion model of the linear theory of binary mixtures of the thermoelastic solids. They have considered a class of boundary value problems and shown uniqueness results. Various composites that are used in several industrial applications occur as multiphase mixtures. These can be treated as interacting continua. The first thermomechanical theory for mixtures of Newtonian fluids in which the two constituents have different temperatures was presented by Eringen and Ingram [18, 25]. One can see the hierarchy of models in the context of mixture theory in [32]. [20] considered the one dimensional problem of two thermoelastic mixtures with two different temperatures. The displacement of each of the phases is assumed to be governed by a linear elasticity equation (which is hyperbolic) with the

relative displacement of the two phases appearing in individual phase equations obeying Newton's third law. Further, the individual phase temperatures also appear in the solid phase displacement equation. The temperature fields obey the energy balance equation which is parabolic in nature. Each of the energy balance equation is coupled to the temperature of the other phase and also the corresponding phase velocity of the solid phases. The coupled system is reformulated as a variational problem and the corresponding existence and uniqueness results are discussed. A finite element approximation of the problem is developed and some a priori error estimates are given followed by some numerical simulations.

Applying heat to human tissue is a well-known treatment mechanism for specific health conditions. Experimental investigations show oscillatory temperature responses when supplying abrupt constant energy to tissue [39]. The non-homogeneous nature of the tissue supports that the heat exchange between blood and tissues always happens at a finite speed. This led to the development of different mathematical models to evaluate the thermal behaviour taking place in living tissues [38]. Estimating the thermoelastic deformation caused by the elevated temperature during thermal ablation procedures is very important to treat cancer. Typical stress-strain equations for an elastic material with thermal load can be thought of as an elementary model for this purpose, which is termed as thermoelastic wave equation [29]. In [40], nonlinear characteristics of bio-heat transfer in deformed soft tissues with thermal expansion/shrinkage are analyzed via a thermo-visco-hyperelastic model. They developed an efficient solution method for solving the coupled model in different computational domains. The solution method is then used to simulate thermal ablation in the liver [38] have proposed a generalized thermo-elastic model involving a dual-phase-lag model of bioheat transfer to model the thermal response of skin tissue. The thermo-elastic response of skin tissue subjected to sudden heating on its boundary is solved by this analytical approach. They have evaluated the contribution of heat-induced stress on thermal pain. [7] investigated the thermo-visco-elastic behavior of tumorous and healthy bovine liver tissue treating the tissue as viscoelastic. They have performed experimental tests and compared them with numerical simulations. Under specific power dissipation conditions, the results of the experimental tests are found to be in good agreement with results of the numerical solution, with experimental results slightly under performing the numerical solution.

We are proposing and investigating a linear hydrodynamic thermo-elasticity system in the context of mixture models where the mixture consists of a fluid and a solid phase. Our main motivating application is biological tissues especially related to tumour growth; although at this time our model does not include any description of this growth. As a first step, we aim to understand better the interplay of thermal coupling with the hydrodynamics on short-time scales where the tumour is essentially stable. This follows the same line of reasoning as in [2, 1]. We point out, that this type of model also comes up in porous media more generally so it is not restricted to this application.

We show that this coupled system has a unique weak solution, where the main difficulty is navigating the different coupling mechanisms in the system. This analysis is done by combining standard existence results for elliptic PDEs with the theory for implicit parabolic PDEs ([33]). Moreover, we analyze the system using a simplified 1D Cartesian coordinate framework and consider a small timescale. A small timescale reduces the two-way coupling of the elasto-hydrodynamic governing equations into the one-way coupling. However, the thermodynamic governing equations remain two-way coupled. Focusing on a one-dimensional setup reduces the complexity allowing for semi-analytical approach to analyze the underlying elasto-thermodynamics. As a next step, we plan to further investigate this system by looking at larger time scales where both the growth of the tumour as well as some nonlinear material relationships have to be considered.

This manuscript is structured as follows: In section 2, we introduce the mathematical model we are considering, perform a non-dimensionalization, and introduce the corresponding weak forms. This is followed by section 3, where we tend to the analysis of the weak form and show that there is a unique weak solution. In section 4, we calculate and present exact solutions in some simplified scenarios (1D Cartesian coordinates, isotropic permeability, time-independent) and go in section 5 to discuss some rudimentary numerical results mainly aimed at highlighting how the different involved mechanism interact with each other. Finally, we end with a short conclusion in section 6.

## 2 Mathematical Model and Setting

In this section, we provide the mathematical model that we are considering in this work and present mathematical framework in which we analyze this model. In the following, let  $\Omega \subset \mathbb{R}^d$ ,  $d = 1, 2, 3$ , denote a bounded Lipschitz

domain with outer unit normal vector  $n$  that represents the tumor region and let  $S = (0, T)$  be the time interval of interest. We introduce a partition of the boundary  $\Gamma, \Gamma_N \subset \partial\Omega$  such that  $|\Gamma| > 0$  and  $\Gamma \cap \Gamma_N = \emptyset$ .

We consider a bi-phasic mixture model for a porous tumor comprising of a solid phase (tumour tissue) and a liquid phase (extracellular fluid) where the main assumption is that both phases are present at every point. For more details regarding this general modeling approach, we refer to [9, 37], but in short: all relevant quantities, e.g., fluid and solid mass densities, are assumed to be defined in all of  $\Omega$  and the exchange of momentum, mass, and heat between the two phases is accounted for via additional exchange terms in the corresponding balance equations. This is an established starting point for the mathematical modelling of, in particular, tissue mechanics, see, e.g., [10, 14]. In the following, we denote with subscripts  $f$  and  $s$  the various physical variables corresponding to the fluid phase and solid phase respectively. For multi-phase systems, we refer to [6, 21].

Symbol	Quantity	Units
$\rho_i$	Mass densities	kg/m <sup>3</sup>
$\mu_i$	2nd Lamé parameter	kg/(m s <sup>2</sup> )
$\lambda_f, \chi_s$	1st Lamé parameter	kg/(m s <sup>2</sup> )
$\varphi_i$	Volume fractions	1
$K$	Drag coefficient	m <sup>2</sup> /s
$b_i$	Body force densities	kg/(m <sup>2</sup> s <sup>2</sup> )
$S_f(P)$	Fluid phase generation	1/s
$c_i$	Specific heat capacity	m <sup>2</sup> /(K s <sup>2</sup> )
$\kappa_i$	Heat conductivity	kg m/(s <sup>3</sup> K)
$\alpha$	Heat exchange coefficient	kg/(m s <sup>3</sup> K)
$\gamma_i$	Modulus of heat dissipation	kg/(m s <sup>2</sup> )
$g_i$	Heat production density	kg/(m s <sup>3</sup> )

**Table 1:** List of model parameters with symbols and units

Now, let  $\mathbf{V}_f$  and  $\mathbf{V}_s$  denote the interstitial fluid velocity (IFV) and the velocity of the solid phase (SPV), respectively. In addition, we introduce the volume fractions  $\varphi_i$  ( $i = s, f$ ), the apparent densities  $\tilde{\rho}_i$ , and the true densities  $\rho_i = \varphi_i \tilde{\rho}_i$ . The mass balance equations are then given via

$$\partial_t(\rho_i) + \nabla \cdot (\rho_i \mathbf{V}_i) = \tilde{\rho}_i S_i,$$

where the  $S_i$  account for the potential mass exchange between the two phases (as a consequence of, e.g., adsorption processes). Similarly, the momentum balance equations can be stated as

$$\rho_i \left( \frac{\partial \mathbf{V}_i}{\partial t} + (\nabla \mathbf{V}_i) \mathbf{V}_i \right) = \nabla \cdot \mathbf{T}_i + \mathbf{b}_i + \mathbf{\Pi}_i.$$

Here,  $\mathbf{T}_i$  are the Cauchy stress tensors,  $\mathbf{b}_i$  volume force densities, and  $\mathbf{\Pi}_i$  account for the exchange of momentum between the phases. By Newton's third law this necessitates  $\mathbf{\Pi}_f = -\mathbf{\Pi}_s$ . Moreover, postulating angular momentum balance in a non-polar setting (in particular, no exchange of angular momentum between the phases), we additionally get symmetry of stress tensors, i.e.,  $\mathbf{T}_i = \mathbf{T}_i^T$ . For the more complex situation allowing for angular momentum coupling, we refer to [15]. Finally, the abstract balance equations for the heat energy read as

$$\rho_i (\partial_t e_i + \nabla e \cdot \mathbf{V}_i) + \nabla \cdot q_i = h_i + \Sigma_i$$

Here,  $e_i$  denote the densities of internal energy,  $q_i$  the heat flux density vectors,  $h_i$  the volume source densities, and  $\Sigma_i$  account for the exchange of heat energy between the phases.

These abstract balance equations, which are in principle valid in a wide range of situations, have to be completed with constitutive relations adapted to the particular setting we have in mind. We start by introducing some additional variables, namely the solid deformation  $\mathbf{U}_s$  which satisfies  $\partial_t \mathbf{U}_s = \mathbf{V}_s$ , the pressure  $P$ , and temperatures  $\theta_f$  and  $\theta_s$ . We work with the overall pressure  $P$  (instead of separate phase pressures) as is usually done in mixture theory, e.g., [3, 30]. The system we consider this work is formulated with respect to these variables  $(\mathbf{V}_f, \mathbf{U}_s, P, \theta_f, \theta_s)$ . In some cases, the evolution of the volume fractions  $\varphi_i$  is also taking into account as part of the overall problem (e.g., [10, 13]).

Assuming the apparent densities to be constant in space and time and the mixture saturation close to constant (that is  $\varphi_f + \varphi_s \approx \text{const.}$ ), summing the two mass balance equations yields

$$\nabla \cdot (\rho_f \mathbf{V}_f + \rho_s \mathbf{V}_s) = S_f + S_s.$$

In a closed system, we would have  $S_f + S_s = 0$ . Generally speaking, the time scale of the tumor growth is significantly larger than for the interstitial fluid processes we are considering [8, 28]. For this reason, we let  $S_s = 0$ . The fluid mass source, on the other hand, is usually assumed to be driven by the average *transmural* pressure (the pressure difference with the vascular space), which takes the form

$$S_f = a_0(P_a - P)$$

where  $P_a$  denotes some ambient pressure, see [13, 28].

We assume that the fluid phase behaves like a *Newtonian* fluid and that the solid stresses can be described with linear thermoelasticity coupled with an additional pressure stress due to the fluid phase:

$$\mathbf{T}_f = -\varphi_f P \mathbb{I} + \lambda_f \nabla \cdot \mathbf{V}_f \mathbb{I} + 2\mu_f D(\mathbf{V}_f), \quad (1)$$

$$\mathbf{T}_s = -\varphi_s P \mathbb{I} + \chi_s \nabla \cdot \mathbf{U}_s \mathbb{I} + 2\mu_s D(\mathbf{U}_s) - \alpha_s \theta_s \mathbb{I}. \quad (2)$$

Here,  $D(\mathbf{v}) = 1/2(\nabla \mathbf{v} + \nabla \mathbf{v}^T)$  denotes the symmetrized gradient,  $\lambda_f$  and  $\mu_f$  the first and second coefficients of viscosity, and  $\chi$  and  $\mu_s$  the elasticity coefficients. Finally,  $\alpha_s$  is the thermal expansion coefficient of the solid phase. Similar constitutive laws without the thermal part can be found in [3, 10]; for the linear thermoelasticity, we refer to [26]. The momentum exchange is assumed to be driven primarily by the difference in velocities (see, e.g., [10, 13, 3] for more details), that is

$$\mathbf{\Pi}_f = -\mathbf{\Pi}_s = \frac{1}{K}(\partial_t \mathbf{U}_s - \mathbf{V}_f)$$

with  $1/K$  denoting the drag coefficient. Finally, the motion of the constituents is assumed to be slow enough such that inertial terms can be neglected. Consequently, the momentum balance equations for the two phases take the form of a coupled system of quasi-stationary elliptic PDEs:

$$-\nabla \cdot (2\mu_f D(\mathbf{V}_f) + \lambda_f \nabla \cdot \mathbf{V}_f \mathbb{I} - \varphi_f P \mathbb{I}) + \frac{1}{K}(\mathbf{V}_f - \partial_t \mathbf{U}_s) = \mathbf{b}_f \quad \text{in } S \times \Omega, \quad (3a)$$

$$-\nabla \cdot (2\mu_s D(\mathbf{U}_s) + \chi_s \nabla \cdot \mathbf{U}_s \mathbb{I} - \varphi_s P \mathbb{I} - \alpha_s \theta_s \mathbb{I}) - \frac{1}{K}(\mathbf{V}_f - \partial_t \mathbf{U}_s) = \mathbf{b}_s \quad \text{in } S \times \Omega, \quad (3b)$$

$$\nabla \cdot (\varphi_f \mathbf{V}_f) + a_0 P = a_0 P_a \quad \text{in } S \times \Omega. \quad (3c)$$

At the outer boundary, we assume the solid part to be clamped and the fluid phase to obey a non-slip condition at one part of the boundary mixed with a (potentially non-homogeneous) Neumann boundary condition on the remaining part:

$$\mathbf{U}_s = 0 \quad \text{on } S \times \partial\Omega, \quad (3d)$$

$$\mathbf{V}_f = 0 \quad \text{on } S \times \Gamma, \quad (3e)$$

$$(2\mu_f D(\mathbf{V}_f) + \lambda_f \nabla \cdot \mathbf{V}_f \mathbb{I} - \varphi_f P \mathbb{I}) \cdot \mathbf{n} = \mathbf{g} \quad \text{on } S \times \Gamma_N. \quad (3f)$$

Here,  $g: S \times \Gamma_N \rightarrow \mathbb{R}^3$  denotes potential forces acting on the fluid via the surface  $\Gamma_N$ .

The heat model considered in this work is based on the principles of linear thermoelasticity, structurally identical to poroelasticity [26, 34]. Here, the internal energies are linear functions of the temperatures, i.e.,

$$e_i = c_i \theta_i$$

where  $c_i > 0$  denote the specific heat capacities of the phases. The heat flux densities are given via *Fourier's law of conductivity*

$$q_f = -\kappa_f \nabla \theta_f + \rho_f c_f \theta_f \mathbf{V}_f, \quad q_s = -\kappa_s \nabla \theta_s$$

with conductivity matrices  $\kappa_i \in \mathbb{R}^{d \times d}$ . Here, we neglect convection in the solid phase. Assuming a linear heat exchange law of Newton type, i.e.,  $h(\theta_f - \theta_s)$ , as well as a linear dissipation law ( $\gamma_i \nabla \cdot \mathbf{V}_i$ ), we end up with

$$\rho_f c_f \partial_t \theta_f - \kappa_f \nabla^2 \theta_f + \rho_f c_f \nabla \cdot (\theta_f \mathbf{V}_f) + h(\theta_f - \theta_s) = -\gamma_f \nabla \cdot \mathbf{V}_f + g_f \quad \text{in } S \times \Omega, \quad (3g)$$

$$\rho_s c_s \partial_t \theta_s - \kappa_s \nabla^2 \theta_s - h(\theta_f - \theta_s) = -\gamma_s \nabla \cdot \partial_t \mathbf{U}_s + g_s \quad \text{in } S \times \Omega. \quad (3h)$$

The parameter  $h$  is the heat exchange coefficient and  $\gamma_i$  is the moduli of heat dissipation. Finally,  $g_i$  denotes the heat production densities. We complete the system with the initial conditions

$$\theta_f(0) = \theta_s(0) = \theta_0 \quad \text{in } \Omega, \quad (3i)$$

and homogeneous Dirichlet boundary conditions

$$\theta_f = \theta_s = 0 \quad \text{on } S \times \partial\Omega. \quad (3j)$$

Of course, other types of boundary conditions, in particular Neumann and Robin exchange conditions, are also reasonable here. The mathematical model describing the hydrodynamics with thermo-elastic effects is then given by eqs. (3a) to (3j).

## 2.1 Nondimensionalization

We use the following transformations to derive a non-dimensionalized form of the governing equations:

$$\begin{aligned} \mathbf{x} &= L\hat{\mathbf{x}}, & \nabla &= \frac{1}{L}\hat{\nabla}, & D &= \frac{1}{L}\hat{D}, & \mathbf{V}_f &= V\hat{\mathbf{V}}_f, & P &= \frac{\mu_f V}{L}\hat{P}, \\ t &= \frac{L}{V}\hat{t}, & \theta_{f,s} &= W_{f,s}\hat{\theta}_{f,s}, & \mathbf{b}_{f,s} &= \mathbf{F}_{f,s}\hat{\mathbf{b}}_{f,s}, & \mathbf{U}_s &= \frac{\mu_f V}{\mu_s}\hat{\mathbf{U}}_s, & g_{f,s} &= G_{f,s}\hat{g}_{f,s}. \end{aligned}$$

In the above transformation, we use certain characteristics quantities, namely, length  $L$ , velocity  $V$ , pressure  $\frac{\mu_f V}{L}$ , temperature  $W$ , force  $F$ , displacement  $\frac{\mu_f V}{\mu_s}$  and potential force  $G$ . Here are the governing equations in the non-dimensionalized form:

$$-\nabla \cdot (2D(\mathbf{V}_f) + (\lambda_1(\nabla \cdot \mathbf{V}_f) - \varphi_f P)\mathbb{I}) + \frac{1}{Da} \left( \mathbf{V}_f - \zeta \frac{\partial \mathbf{U}_s}{\partial t} \right) = \mathbf{b}_f \quad \text{in } S \times \Omega, \quad (4a)$$

$$-\nabla \cdot (2D(\mathbf{U}_s) + (\lambda_2(\nabla \cdot \mathbf{U}_s) - \varphi_s P - \delta_s \theta_s)\mathbb{I}) - \frac{1}{Da} \left( \mathbf{V}_f - \zeta \frac{\partial \mathbf{U}_s}{\partial t} \right) = \mathbf{b}_s \quad \text{in } S \times \Omega, \quad (4b)$$

$$\nabla \cdot (\varphi_f \mathbf{V}_f) + a_1 P = a_2 \quad \text{in } S \times \Omega. \quad (4c)$$

Boundary conditions:

$$\mathbf{U}_s = 0 \quad \text{on } S \times \partial\Omega, \quad (4d)$$

$$\mathbf{V}_f = 0 \quad \text{on } S \times \Gamma, \quad (4e)$$

$$\left( 2D(\mathbf{V}_f) + (\lambda_1(\nabla \cdot \mathbf{V}_f) - \varphi_f P)\mathbb{I} \right) \cdot \mathbf{n} = \mathbf{g} \quad \text{on } S \times \Gamma_N. \quad (4f)$$

$$\text{Pe}_f \left( \frac{\partial \theta_f}{\partial t} + \nabla \cdot (\theta_f \mathbf{V}_f) \right) - \nabla^2 \theta_f = -N(\theta_f - W\theta_s) - \delta'_f \nabla \cdot \mathbf{V}_f + g_f \quad \text{in } S \times \Omega, \quad (4g)$$

$$\text{Pe}_s \frac{\partial \theta_s}{\partial t} - \nabla^2 \theta_s = -\kappa N \left( \theta_s - \frac{1}{W} \theta_f \right) - \delta'_s \nabla \cdot \partial_t \mathbf{U}_s + g_s \quad \text{in } S \times \Omega \quad (4h)$$

Initial conditions:

$$\theta_f(0) = \theta_s(0) = \theta_0 \quad \text{in } \Omega, \quad (4i)$$

Boundary conditions:

$$\theta_f = \theta_s = 0 \quad \text{on } S \times \partial\Omega. \quad (4j)$$

Non-dimensional parameters	Description
$Da = \frac{\mu_f K}{L^2}$	Darcy number
$a_1 = a_0 \mu_f, a_2 = \frac{a_0 P_a L}{V}$ ,	some non-dimensionalized constants
$\lambda_1 = \frac{\lambda_f}{\mu_f}, \lambda_2 = \frac{\lambda_s}{\mu_s}$	ratios of viscosity parameters
$\delta_s = \frac{L \alpha_s W_s}{V \mu_f}$	Ratio of thermal expansion to the viscous forces
$Pe_f = \frac{\rho_f c_f L^2 V}{\kappa_f L}$	Peclet number in fluid phase
$Pe_s = \frac{\rho_s c_s L^2 V}{\kappa_s L}$	Peclet number in solid phase
$N = \frac{h L^2}{\kappa_f}$	Nondimensionalized thermal exchange parameter
$\kappa = \frac{\kappa_f}{\kappa_s}, W = \frac{W_s}{W_f}$	Ratio of heat conductivities
$\delta'_f = \frac{L \gamma_f V}{\kappa_f W_f}, \delta'_s = \frac{\gamma_s V^2 \mu_f}{\mu_s \kappa_s W_s}$ ,	Some non-dimensionalized constants
$\zeta = \frac{V \mu_f}{\mu_s L}$	Ratio of viscous forces to the shear stress

Table 2: List of non-dimensional parameters

## 2.2 Variational formulation

We introduce the Hilbert spaces

$$\begin{aligned} \mathbf{H}_0^1(\Omega) &:= H^1(\Omega)^d, \\ \mathbf{H}_\Gamma^1(\Omega) &:= \{u \in H^1(\Omega)^d : u = 0 \text{ on } \Gamma\}, \\ \mathcal{W}(S, \Omega) &:= \{\theta \in L^2(S; H_0^1(\Omega)) : \partial_t \theta \in L^2(S; H^{-1}(\Omega))\}. \end{aligned}$$

Please note that Korn's inequality [16, Theorem 3.1] together with Poincaré's inequality ensures that there is  $C > 0$  such that

$$\|u\|_{\mathbf{H}_0^1(\Omega)} \leq C \|D(u)\|_{L^2(\Omega)}, \quad \|v\|_{\mathbf{H}_\Gamma^1(\Omega)} \leq C \|D(v)\|_{L^2(\Omega)}. \quad (5)$$

In the following, we use  $\langle \cdot, \cdot \rangle_V$  to denote the dual product between  $V$  and its dual  $V^*$ . A weak form of the hydromechanics part, eqs. (3a) to (3f), is given via

$$\int_{\Omega} \mathcal{A}_f D(V_f) : D(W_f) - \varphi_f P \nabla \cdot W_f + \frac{1}{K} V_f \cdot W_f \, dx = \int_{\Omega} f_f \cdot W_f \, dx + \int_{\Gamma_N} f_N \cdot W_f \, d\sigma, \quad (6a)$$

$$\int_{\Omega} \mathcal{A}_s D(U_s) : D(W_s) - (\varphi_s P + \gamma_s \theta_s) \nabla \cdot W_s + \frac{V_f \cdot W_s}{K} \, dx = \int_{\Omega} f_s \cdot W_s \, dx, \quad (6b)$$

$$\int_{\Omega} (\phi_f \nabla \cdot V_f - a_0 (P_a - P)) Q \, dx = 0, \quad (6c)$$

which is assumed to hold for almost all  $t \in S$  and for all test functions

$$(W_f, W_s, Q) \in \mathbf{H}_\Gamma^1(\Omega) \times \mathbf{H}_0^1(\Omega) \times L^2(\Omega).$$

For ease of notation, we have introduced the fourth-rank tensors  $A_i \in \mathbb{R}^{d \times d \times d \times d}$  via<sup>1</sup>

$$(A_i)_{klmn} = \mu_i (\delta_{km} \delta_{ln} + \delta_{kn} \delta_{lm}) + \lambda_i \delta_{kl} \delta_{mn}.$$

The variational form for the thermo part (given by eqn. eqs. (3g) to (3j)) takes the form

$$\begin{aligned} & - \int_S \int_{\Omega} \rho_f c_f \theta_f \partial_t \psi_f \, dx \, dt + \int_S \int_{\Omega} \gamma_f \nabla \cdot V_f \psi_f \, dx \, dt \\ & + \int_S \int_{\Omega} \kappa_f \nabla \theta_f \cdot \nabla \psi_f \, dx \, dt - \int_S \int_{\Omega} \rho_f c_f \theta_f V_f \cdot \nabla \psi_f \, dx \, dt \\ & + \int_S \int_{\Omega} \alpha (\theta_f - \theta_s) \psi_f \, dx \, dt = \int_S \int_{\Omega} g_f \psi_f \, dx \, dt + \int_{\Omega} \theta_0 \psi_f(0) \, dx, \quad (6d) \end{aligned}$$

<sup>1</sup>Here,  $\delta_{ij}$  is the Kronecker delta.

$$\begin{aligned}
& - \int_S \int_\Omega \rho_s c_s \theta_s \partial_t \psi_s \, dx \, dt - \int_S \int_\Omega \gamma_s \nabla \cdot U_s \partial_t \psi_s \, dx \, dt + \int_S \int_\Omega \kappa_s \nabla \theta_s \cdot \nabla \psi_s \, dx \, dt \\
& + \int_S \int_\Omega \alpha (\theta_s - \theta_f) \psi_s \, dx \, dt = \int_S \int_\Omega g_s \psi_s \, dx \, dt + \int_\Omega (\theta_0 + \gamma_s \nabla \cdot U_s(0)) \psi_s(0) \, dx \quad (6e)
\end{aligned}$$

for all test functions

$$\psi_f, \psi_s \in W.$$

One potential problem in eq. (6e) is the regularity of  $U_s$  with respect to time. As eq. (6b) is only supposed to hold true for almost all  $t \in S$ , it is a priori unclear how to interpret the initial condition  $\nabla \cdot U_s(0)$ . To circumvent this particular problem, we will employ higher regularity of the hydrodynamic data  $f_s, f_f, g$ .

**Remark.** Please note that by employing a less restrictive notion of a weak solution where the initial condition is obtained via

$$\lim_{t \rightarrow 0} (\theta_s(t) + \gamma_s \nabla \cdot U_s(t))$$

these regularity concerns can be relaxed. In this setting, both  $\theta_f$  and  $\nabla \cdot U_s$  may not have a weak time derivative as only  $\partial_t (\rho_s c_s \theta_s + \gamma_s \nabla \cdot U_s) \in L^2(S; H^{-1}(\Omega))$  is required. We refer to [34] where this idea is explored in more detail in the context of poroelasticity.

We provide a short summary of the main regularity assumptions:

- (A1) **Geometry:**  $\Omega \subset \mathbb{R}^d$  is a bounded Lipschitz domain with outer normal vector  $n$ .
- (A2) **Data:**  $f_f, f_s \in L^2(S \times \Omega)^d$ ,  $g_f, g_s \in L^2(S \times \Omega)$ ,  $f_N \in L^2(S \times \Gamma_N)$ .
- (A3) **Time-regularity of data:**  $\partial_t f_f \in L^2(S; (\mathbf{H}_T^1(\Omega))^*)$ ,  $\partial_t f_N \in L^2(S \times \Gamma_N)$ , and  $\partial_t f_s \in L^2(S; \mathbf{H}^{-1}(\Omega))$
- (A4) **Coefficients:** Positive coefficients  $\mu_i, \lambda_i, \varphi_i, \rho_i, c_i, \gamma_i, \kappa_i$  ( $i = f, s$ ),  $\alpha, K$

### 3 Well-posedness

In this section, we tend to the mathematical analysis of the fully coupled problem with quasi-static hydrodynamics that is given by eqs. (3a) to (3j). Our approach here is partially motivated by [34] where a somewhat similar structure to our thermo-elasticity coupling is considered in the context of poroelasticity, although without the mixture component and with different coupling mechanisms. We also refer to [17] where the analysis of a thermo-elasticity model is considered. Regarding the general strategy we employ, the analysis of this linear but highly coupled system is done in two parts:

- 1) We first look at the hydrodynamics sub-problem given by eqs. (6a) to (6c) for prescribed temperature profiles. This is done in the context of standard elliptic theory. The main result here is given by lemma 1.
- 2) Using the resulting solution operator, we tackle the complete coupled problem. In this part, we are relying on results on implicit partial differential equations as presented in [33]. See theorem 1.

#### 3.1 Hydrodynamics

We first focus on the hydrodynamics part given by eqs. (6a) to (6c) with some prescribed temperature function  $\vartheta_s \in L^2(\Omega)$ . Making explicit use of eq. (6c), we see that

$$a_0 P = -\varphi_f \nabla \cdot V_f + a_0 P_a \quad \text{in } L^2(\Omega). \quad (7)$$

Substituting eq. (7) into eqs. (6a) and (6b), we are therefore able to decouple the pressure function from the fluid velocity. By noting that

$$\int_\Omega \nabla \cdot W_f \, dx = \int_{\Gamma_N} W_f \cdot n \, d\sigma \quad (W_f \in \mathbf{H}_T^1(\Omega)), \quad \int_\Omega \nabla \cdot W_s \, dx = 0 \quad (W_s \in \mathbf{H}_0^1(\Omega)),$$

we arrive at the following problem: Find  $(V_f, U_s) \in \mathbf{H}_\Gamma^1(\Omega) \times \mathbf{H}_0^1(\Omega)$  such that

$$\int_{\Omega} A_f D(V_f) : D(W_f) + \frac{\varphi_f^2}{a_0} \nabla \cdot V_f \nabla \cdot W_f + \frac{1}{K} V_f \cdot W_f \, dx = \int_{\Omega} f_f \cdot W_f \, dx + \int_{\Gamma_N} (f_N + P_\alpha) \cdot W_s \, d\sigma, \quad (8a)$$

$$\int_{\Omega} A_s D(U_s) : D(W_s) + \left( \frac{\varphi_s \varphi_f}{\alpha_0} \nabla \cdot V_f - \gamma_s \vartheta \right) \nabla \cdot W_s + \frac{1}{K} V_f \cdot W_s \, dx = \int_{\Omega} f_s \cdot W_s \, dx \quad (8b)$$

for all  $(W_f, W_s) \in \mathbf{H}_\Gamma^1(\Omega) \times \mathbf{H}_0^1(\Omega)$ . From here the pressure function can then be recovered via eq. (7). For a more compact operator formulation of this system, we introduce elliptic operators

$$\mathcal{A}_f : \mathbf{H}_\Gamma^1(\Omega) \rightarrow (\mathbf{H}_\Gamma^1(\Omega))^*, \quad \mathcal{A}_s : \mathbf{H}_0^1(\Omega) \rightarrow \mathbf{H}^{-1}(\Omega)$$

via

$$\langle \mathcal{A}_f v, w \rangle_{\mathbf{H}_\Gamma^1(\Omega)} = \int_{\Omega} A_f D(v) : D(w) \, dx + \frac{\varphi_f^2}{a_0} \nabla \cdot v \nabla \cdot w + \frac{1}{K} v w \, dx, \quad (9a)$$

$$\langle \mathcal{A}_s u, w \rangle_{\mathbf{H}_0^1(\Omega)} = \int_{\Omega} A_s D(u) : D(w) \, dx. \quad (9b)$$

In addition, we introduce coupling operators

$$\mathcal{B} : \mathbf{H}_\Gamma^1(\Omega) \rightarrow \mathbf{H}^{-1}(\Omega), \quad \nabla : L^2(\Omega) \rightarrow \mathbf{H}^{-1}(\Omega)$$

defined via

$$\langle \mathcal{B} v, w \rangle_{\mathbf{H}_0^1(\Omega)} = \int_{\Omega} \frac{\varphi_s \varphi_f}{\alpha_0} \nabla \cdot v \nabla \cdot w + \frac{1}{K} v w \, dx, \quad (9c)$$

$$\langle \nabla \pi, w \rangle_{\mathbf{H}_0^1(\Omega)} = - \int_{\Omega} \gamma_s \pi \nabla \cdot w \, dx \quad (9d)$$

as well as the right-hand side operator

$$\mathcal{F}_f \in (\mathbf{H}_\Gamma^1(\Omega))^*, \quad \langle \mathcal{F}_f, w \rangle = \int_{\Omega} f_f \cdot w \, dx + \int_{\Gamma_N} (f_N + P_\alpha) \cdot w \, d\sigma. \quad (9e)$$

With this, the weak form given by eqs. (8a) and (8b) can alternatively be expressed as an abstract operator problem: For  $\vartheta \in L^2(\Omega)$ , find  $V_f \in \mathbf{H}_\Gamma^1(\Omega)$  and  $U_s \in \mathbf{H}_0^1(\Omega)$  such that

$$\begin{aligned} \mathcal{A}_f V_f &= \mathcal{F}_f \quad \text{in } (\mathbf{H}_\Gamma^1(\Omega))^*, \\ \mathcal{A}_s U_s + \mathcal{B} V_f + \nabla \vartheta &= f_s \quad \text{in } \mathbf{H}^{-1}(\Omega). \end{aligned}$$

In the following lemma, we establish that this system of linear elliptic PDEs has a unique solution.

**Lemma 1.** *Let  $f_f, f_s \in L^2(\Omega)$  and  $f_N \in L^2(\Gamma_N)$ . For every  $\vartheta_s \in L^2(\Omega)$ , there is a unique solution  $(V_f, U_s) \in \mathbf{H}_\Gamma^1(\Omega) \times \mathbf{H}_0^1(\Omega)$  to the problem given by eqs. (8a) and (8b). The corresponding pressure function  $P \in L^2(\Omega)$  is then given by eq. (7). Moreover, the solution satisfies energy estimates of the form*

$$\|V_f\|_{\mathbf{H}_\Gamma^1(\Omega)} \leq C \left( \|f_f\|_{L^2(\Omega)} + \|f_N + P_\alpha\|_{L^2(\Gamma_N)} \right), \quad (10a)$$

$$\|U_s\|_{\mathbf{H}_0^1(\Omega)} \leq C \left( \|\vartheta\|_{L^2(\Omega)} + \|f_f\|_{L^2(\Omega)} + \|f_s\|_{L^2(\Omega)} + \|f_N + P_\alpha\|_{L^2(\Gamma_N)} \right) \quad (10b)$$

where  $C > 0$  is independent of  $\vartheta$ .



*Proof.* The operator  $\mathcal{A}_f$  is linear, continuous, and coercive since all coefficients are positive and the applicability of Korn's inequality eq. (5). As a consequence, we can follow via the Lemma of Lax-Milgram that there is a unique solution  $V_f$  such that

$$\mathcal{A}_f V_f = \mathcal{F}_f \quad \text{in } (\mathbf{H}_\Gamma^1(\Omega))^*,$$

or, more explicitly,

$$V_f = \mathcal{A}_f^{-1} \mathcal{F}_f \quad \text{in } \mathbf{H}_\Gamma^1(\Omega), \quad (11)$$

where the inverse operator  $\mathcal{A}_f^{-1} : (\mathbf{H}_\Gamma^1(\Omega))^* \rightarrow \mathbf{H}_\Gamma^1(\Omega)$  is also continuous and coercive.

For the solid phase, we similarly have linearity and continuity of  $\mathcal{A}_s$ . Since it is also coercive by virtue of Korn's inequality eq. (5) and since  $\mathcal{B}$  is a linear and continuous operator, we find a unique  $U_s$  satisfying

$$\mathcal{A}_s U_s + \mathcal{B} V_f = -\nabla \vartheta_s + f_s \quad \text{in } \mathbf{H}^{-1}(\Omega),$$

where  $V_f$  is given by eq. (11). Solving for  $U_s$ , we calculate

$$U_s = \mathcal{A}_s^{-1} \mathcal{B} \mathcal{A}_f^{-1} \mathcal{F}_f - \mathcal{A}_s^{-1} \nabla \vartheta_s + \mathcal{A}_s^{-1} f_s \quad \text{in } \mathbf{H}_0^1(\Omega). \quad (12)$$

Setting  $\tilde{\mathcal{F}} = \mathcal{B} \mathcal{A}_f^{-1} \mathcal{F}_f + f_s \in L^2(\Omega)$ , this amounts to

$$U_s = -\mathcal{A}_s^{-1} \left( \nabla \vartheta_s + \tilde{\mathcal{F}} \right) \quad \text{in } \mathbf{H}_0^1(\Omega).$$

The estimate eq. (10) now can be established via standard energy estimates or alternatively by directly using the continuity of the involved operators: Using the coerciveness of  $\mathcal{A}_s$  and the definition of the  $\nabla$ -operator, we have

$$c \|U_s\|_{\mathbf{H}_0^1(\Omega)}^2 \leq \langle \mathcal{A}_s U_s, U_s \rangle_{\mathbf{H}_0^1(\Omega)} = \int_{\Omega} \gamma_s \vartheta_s \nabla \cdot U_s \, dx + \int_{\Omega} \tilde{\mathcal{F}} \cdot U_s \, dx$$

which leads to (using Young's inequality)

$$\|U_s\|_{\mathbf{H}_0^1(\Omega)}^2 \leq C \left( \|\vartheta\|_{L^2(\Omega)}^2 + \|\tilde{\mathcal{F}}\|_{L^2(\Omega)}^2 \right).$$

The coerciveness of  $\mathcal{A}_f$  and the structure of  $\mathcal{F}_f$  implies

$$c \|\mathcal{A}_f^{-1} \mathcal{F}_f\|_{\mathbf{H}_\Gamma^1(\Omega)}^2 \leq \|\mathcal{F}_f\|_{(\mathbf{H}_\Gamma^1(\Omega))^*}^2 \leq \|f_f\|_{L^2(\Omega)}^2 + \|f_N + P_a\|_{L^2(\Gamma_N)}^2$$

leading to (using the continuity of  $\mathcal{B}$ )

$$\|\tilde{\mathcal{F}}\|_{L^2(\Omega)}^2 \leq C \left( \|f_s\|_{L^2(\Omega)}^2 + \|f_f\|_{L^2(\Omega)}^2 + \|f_N + P_a\|_{L^2(\Gamma_N)}^2 \right).$$

Finally, with eq. (11) the estimate eq. (10) follows.  $\square$

With Lemma 1, we have the existence of a solution operator  $\mathcal{L} : L^2(\Omega) \rightarrow \mathbf{H}_\Gamma^1(\Omega) \times \mathbf{H}_0^1(\Omega)$  mapping a given solid temperature profile  $\theta_s$  to the corresponding hydrodynamic solution  $(V_f, U_s)$ . In the fully-coupled problem (eqs. (6a) to (6e)), the temperature profiles will depend on time as well and so, as a consequence, will the hydrodynamic solution. Moreover, the regularity of  $(V_f, U_s)$  with respect to time is essential for the full problem, specifically for  $U_f$  where we want to make sense of  $\nabla \cdot \partial_t U_s$  (eq. (3h)).

In the following lemma, we collect some important regularity results for the solution  $(V_f, U_s)$  with respect to a time parameter introduced via the data.

**Lemma 2.** *For  $t \in S$ , let  $t \mapsto (f_s(t), f_f(t), f_N(t), \vartheta_s(t))$  denote time-dependent data and let  $t \mapsto (V_f(t), U_s(t))$  be the corresponding time-parametrized solution due to lemma 1.*

(i) *Let  $f_s, f_f, \vartheta_s \in L^2(S \times \Omega)^d$ ,  $f_N \in L^2(S \times \Gamma_N)^d$ . Then,*

$$V_f \in L^2(S; \mathbf{H}_\Gamma^1(\Omega)), \quad U_s \in L^2(S; \mathbf{H}_0^1(\Omega)).$$

(ii) *If  $f_f \in L^\infty(S \times \Omega)^d$  and  $f_N \in L^\infty(S \times \Gamma_N)$ , we also find that  $V_f \in L^\infty(S \times \Omega)^d$ .*

(iii) Let  $\vartheta = 0$ . If  $\partial_t f_f \in L^2(S; (\mathbf{H}_\Gamma^1(\Omega))^*)$ ,  $\partial_t f_N \in L^2(S \times \Gamma_N)$ , and  $\partial_t f_s \in L^2(S; \mathbf{H}^{-1}(\Omega))$  we have

$$\partial_t \nabla \cdot U_s \in L^2(S \times \Omega)^d.$$

*Proof.* (i). The  $L^2$ -time regularity of  $(V_f, U_s)$  transfers in a straightforward way from the data as all involved operators are linear, continuous, and time-independent.

(ii). The  $L^\infty$ -estimates can be shown by testing eq. (8a) with  $V_f^{\pm k} := (V_f - k)_\pm$  for some  $k \in \mathbb{Z}^3$  leading to (with the use of Poincaré's inequality)

$$\|V_f^{\pm k}\|_{\mathbf{H}_\Gamma^1(\Omega)} \leq \langle \mathcal{F}_f, V_f^{\pm k} \rangle_{\mathbf{H}_\Gamma^1(\Omega)}.$$

(iii). With  $\partial_t f_f \in L^2(S; (\mathbf{H}_\Gamma^1(\Omega))^*)$  and  $\partial_t f_N \in L^2(S \times \Gamma_N)$  and taking into account the structure of  $\mathcal{F}_f$  (eq. (9e)), it holds

$$\partial_t \mathcal{F}_f \in L^2(S; (\mathbf{H}_\Gamma(\Omega))^*), \quad \langle \partial_t \mathcal{F}_f(t), w \rangle_{\mathbf{H}_\Gamma(\Omega)} = \langle \partial_t f_f(t), w \rangle_{\mathbf{H}_\Gamma(\Omega)} + \int_{\Gamma_N} \partial_t f_N(t) \cdot w \, dx$$

which implies, via lemma 1,  $\partial_t V_f \in L^2(S; \mathbf{H}_\Gamma(\Omega))$  and, in consequence,  $\partial_t U_s \in L^2(S; \mathbf{H}_0^1(\Omega))$ .  $\square$

### 3.2 Heat problem

We now take a closer look at the thermo system whose weak formulation is given by eqs. (6d) and (6e): Find  $(\theta_f, \theta_s) \in \mathcal{W}^2$  such that

$$\begin{aligned} & - \int_S \int_\Omega \rho_f c_f \theta_f \partial_t \psi_f \, dx \, dt + \int_S \int_\Omega \gamma_f \nabla \cdot V_f \psi_f \, dx \, dt \\ & \quad + \int_S \int_\Omega \kappa_f \nabla \theta_f \cdot \nabla \psi_f \, dx \, dt - \int_S \int_\Omega \rho_f c_f \theta_f V_f \cdot \nabla \psi_f \, dx \, dt \\ & \quad + \int_S \int_\Omega \alpha(\theta_f - \theta_s) \psi_f \, dx \, dt = \int_S \int_\Omega g_f \psi_f \, dx \, dt + \int_\Omega \theta_0 \psi_f(0) \, dx, \\ & - \int_S \int_\Omega \rho_s c_s \theta_s \partial_t \psi_s \, dx \, dt - \int_S \int_\Omega \gamma_s \nabla \cdot U_s \partial_t \psi_s \, dx \, dt + \int_S \int_\Omega \kappa_s \nabla \theta_s \cdot \nabla \psi_s \, dx \, dt \\ & \quad + \int_S \int_\Omega \alpha(\theta_s - \theta_f) \psi_s \, dx \, dt = \int_S \int_\Omega g_s \psi_s \, dx \, dt + \int_\Omega (\theta_0 + \gamma_s \nabla \cdot U_s(0)) \psi_s(0) \, dx \end{aligned}$$

for all test functions

$$\psi_f, \psi_s \in W.$$

In this problem, we have to take care of the heat coupling (given via the heat exchange terms  $\alpha(\theta_s - \theta_f)$ ) as well as the coupling of the heat with the mechanics (in the fluid phase via the convection term  $\nabla \cdot (\rho_f c_f \theta_f V_f)$  and the dissipation term  $\gamma_f \nabla \cdot V_f$  and in the solid phase via the dissipation term  $\gamma_s \partial_t \nabla \cdot U_s$ ).

We first focus on the fluid heat system described by eq. (6d); this one is straightforward as we do not have to deal with the mixed derivative term (time and spatial)  $(\nabla \cdot U_s, \partial_t \varphi_s)_\Omega$  that comes up in the solid heat equation.

**Lemma 3.** Let  $g_f \in L^2(S \times \Omega)$  and  $\theta_0 \in L^2(\Omega)$ . For any  $\vartheta_s \in L^2(S \times \Omega)$  and  $v_f \in L^\infty(S \times \Omega)^3 \cap L^2(S; \mathbf{H}_\Gamma^1(\Omega))$ , there is a unique function  $\theta_f \in \mathcal{W}$  satisfying

$$\begin{aligned} & - \int_S \int_\Omega \rho_f c_f \theta_f \partial_t \psi_f \, dx \, dt + \int_S \int_\Omega \gamma_f \nabla \cdot v_f \psi_f \, dx \, dt \\ & \quad + \int_S \int_\Omega \kappa_f \nabla \theta_f \cdot \nabla \psi_f \, dx \, dt - \int_S \int_\Omega \rho_f c_f \theta_f v_f \cdot \nabla \psi_f \, dx \, dt \\ & \quad + \int_S \int_\Omega \alpha(\theta_f - \vartheta_s) \psi_f \, dx \, dt = \int_S \int_\Omega g_f \psi_f \, dx \, dt + \int_\Omega \theta_0 \psi_f(0) \, dx \end{aligned}$$

for all  $\psi_f \in W$  with  $\psi_f(T) = 0$ . Moreover,

$$\begin{aligned} \|\theta_f\|_{L^\infty(S; L^2(\Omega))}^2 + \|\partial_t \theta_f\|_{L^2(S \times \Omega)}^2 + \|\nabla \theta_f\|_{L^2(S \times \Omega)}^2 \\ \leq C \left( \|\vartheta_s\|_{L^2(S \times \Omega)}^2 + \|g_f\|_{L^2(S \times \Omega)}^2 + \|\theta_0\|_{L^2(\Omega)}^2 + \|v_f\|_{L^\infty(S \times \Omega)}^2 \right) \end{aligned} \quad (13)$$

*Proof.* With given data this is a standard parabolic problem with convection, we refer to [19, Chapter 7.1].  $\square$

Now, let  $V_f$  be the solution given by lemma 1 and the data  $f_f, f_N$  be as regular as required in lemma 2. Then,  $V_f \in L^\infty(S \times \Omega)^d \cap L^2(S; \mathbf{H}_\Gamma^1(\Omega))$  which implies that lemma 3 (taking  $v_f = V_f$ ) is applicable. We introduce the solution operator  $\mathcal{T}_f: L^2(S \times \Omega) \rightarrow \mathcal{W}$  assigning to a function  $\vartheta_s \in L^2(S \times \Omega)$  the corresponding unique solution  $\theta_f \in \mathcal{W}$  given by virtue of Lemma 3 when  $v_f = V_f$ . Note that  $T_f - T_f(0)$  is linear, continuous, and, by Aubin-Lyons-Simon lemma [35], also compact from  $L^2(S \times \Omega)$  to  $L^2(S \times \Omega)$ . In that setting, any solution  $(\theta_f, \theta_s)$  of the thermo-problem eqs. (6d) and (6e) has to satisfy  $\theta_f = \mathcal{T}_f \theta_s$ .

Now, we start with the characterization of  $U_s$  given by eq. (12) via lemma 1 and splitting it in terms of a prescribed solid temperature  $\vartheta$  and data parts, i.e.,

$$U_s(t) = \underbrace{-\mathcal{A}_s^{-1} \nabla \vartheta(t)}_{U_\vartheta(t)} + \underbrace{\mathcal{A}_s^{-1} \left( f_s(t) - \mathcal{B} \mathcal{A}_f^{-1} \mathcal{F}_f(t) \right)}_{U_d(t)} \quad \text{in } \mathbf{H}_0^1(\Omega) \text{ for a.a. } t \in S.$$

When  $f_s, f_f, f_N$  satisfy Assumptions (A2) and (A3), we have  $\partial_t \nabla \cdot U_d \in L^2(S \times \Omega)$  (lemma 2(iii)) and can therefore slightly rearrange eq. (6e) into

$$\begin{aligned} - \int_S \int_\Omega \rho_s c_s \theta_s \partial_t \psi_s \, dx - \int_S \int_\Omega \gamma_s \nabla \cdot \mathcal{A}_s^{-1} \nabla \theta_s \partial_t \psi_s \, dx \, dt \\ + \int_S \int_\Omega \kappa_s \nabla \theta_s \cdot \nabla \psi_s \, dx \, dt + \int_S \int_\Omega \alpha (\theta_s - \mathcal{T}_f \theta_s) \psi_s \, dx \, dt \\ = \int_S \int_\Omega g_s \psi_s \, dx \, dt + \int_\Omega (\theta_0 - \gamma_s \nabla \cdot \mathcal{A}_s^{-1} \nabla \theta_0) \psi_s(0) \, dx + \int_S \int_\Omega \partial_t \nabla \cdot U_d \psi \, dx \, dt \end{aligned}$$

for all  $\varphi_s \in L^2(S; H_0^1(\Omega))$ . Introducing the linear operators

$$\begin{aligned} \mathcal{K}: H_0^1(\Omega) &\rightarrow H^{-1}(\Omega), & \langle \mathcal{K} \vartheta, \varphi \rangle_{H_0^1(\Omega)} &= \int_\Omega \kappa_s \nabla \theta_s \cdot \nabla \psi_s \, dx, \\ \mathcal{R}: L^2(\Omega) &\rightarrow L^2(\Omega), & \mathcal{R} &= \nabla \cdot \mathcal{A}_s^{-1} \nabla, \\ \mathcal{M}: L^2(\Omega) &\rightarrow L^2(\Omega), & \mathcal{M} &= \rho_s c_s \text{Id} + \gamma_s \mathcal{R} \end{aligned}$$

and the data  $\mathcal{G} \in L^2(S \times \Omega)$  given by  $\mathcal{G} = g_s + \partial_t \nabla \cdot U_d$ , the solid-heat system can be abstractly formulated as: For  $\vartheta_f \in L^2(S \times \Omega)$ , find  $\theta_s \in L^2(S; H_0^1(\Omega))$  with  $\partial_t (\mathcal{M} \theta_s) \in L^2(S; H^{-1}(\Omega))$  and such that

$$\partial_t (\mathcal{M} \theta_s) + \mathcal{K} \theta_s + \alpha (\theta_s - \vartheta_f) = \mathcal{G} \quad \text{in } L^2(S; H^{-1}(\Omega)). \quad (14)$$

Moreover, it has to satisfy  $\lim_{t \rightarrow 0} \mathcal{M} \theta_s(t) = \mathcal{M} \theta_0$  in  $L^2(\Omega)$ .

**Lemma 4.** *The linear operator*

$$\mathcal{R}: L^2(\Omega) \rightarrow L^2(\Omega), \quad \mathcal{R} = \nabla \cdot \mathcal{A}_s^{-1} \nabla$$

*is continuous, self-adjoint, and positive.*

*Proof.*  $\mathcal{R}$  is a composition of continuous operators and, as a result, itself continuous. Let  $f, g \in L^2(\Omega)$ . Then,

$$\int_\Omega \mathcal{R} f g \, dx = \langle \nabla g, \mathcal{A}_s^{-1} \nabla f \rangle_{\mathbf{H}_0^1(\Omega)}.$$

Since  $\mathcal{A}_s^{-1}$  is positive and symmetric, it follows that

$$\int_\Omega \mathcal{R} f g \, dx = \int_\Omega \mathcal{R} g f \, dx$$

as well as

$$\int_{\Omega} \mathcal{R}ff \, dx \geq 0.$$

□

**Lemma 5.** *Let  $\vartheta_f \in L^2(S \times \Omega)$  as well as  $\mathcal{G} \in L^2(S \times \Omega)$  and  $\theta_0 \in L^2(\Omega)$ . Then, there is a unique solution  $\theta_s \in L^2(S; H_0^1(\Omega))$  with  $\partial_t(\mathcal{M}\theta_s) \in L^2(S; H^{-1}(\Omega))$  satisfying  $\lim_{t \rightarrow 0} \mathcal{M}\theta_s(t) = \mathcal{M}\theta_0$  in  $L^2(\Omega)$  as well as the problem eq. (14).*

*Proof.* Observing that  $\mathcal{R}$  is continuous, self-adjoint, and positive and  $\mathcal{K}$  is coercive, the result for this implicit parabolic PDE follows from [33, Chapter III, Proposition 3.2]. □

With these results, we can now prove the general well-posedness:

**Theorem 1 (Existence result).** *Let Assumptions (A1)–(A4) be satisfied. There exists a unique weak solution  $V_f \in L^2(S; \mathbf{H}_\Gamma^1(\Omega))$ ,  $U_s \in C^1(\bar{S}; \mathbf{H}_0^1(\Omega))$ , and  $\theta = (\theta_f, \theta_s) \in \mathcal{W}(S, \Omega)^2$  solving System eq. (3) in the sense of eqs. (6a) to (6e).*

*Proof.* With lemma 5, we get  $V_f \in L^2(S; \mathbf{H}_\Gamma^1(\Omega))$ ,  $U_s \in C^1(\bar{S}; \mathbf{H}_0^1(\Omega))$ , and  $\theta_s \in \mathcal{W}(S, \Omega)$ , and with lemma 3, we can then find the corresponding fluid temperature profile  $\theta_f \in \mathcal{W}(S, \Omega)$ . □

## 4 Reduced model

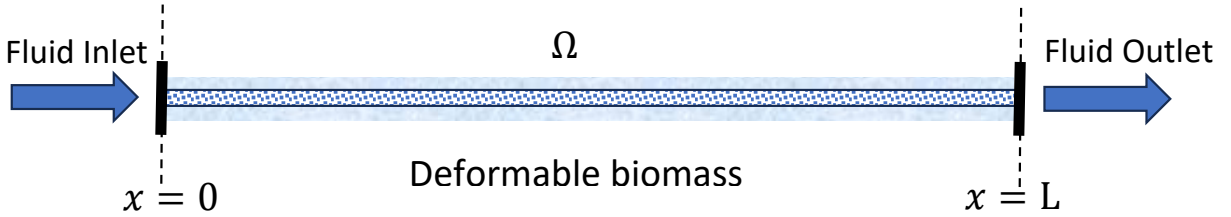


Figure 1: Schematic representation of the 1D model.

So far we have proposed a complex coupled model of thermo-elasto-hydrodynamics and shown corresponding existence and uniqueness results. The weak formulation setting may enable the development of numerical solutions via discretization methods like the Galerkin method. However, as the first steps, in this section, we wish to obtain the semi-analytical solution of the non-dimensional equations (4a-4h). Note that we consider infinitesimal deformation of the solid phase in the analysis to retain linear dependence of the solid stress tensor. We further assume that the solid deformation is independent of time, i.e.  $\partial U_s / \partial t = 0$ . Moreover, the body force densities and the heat production densities are neglected. We assume a sufficiently short timescale that allows us to neglect the time dependency of the temperature in the solid and fluid phases. Moreover, the mean temperature to non-dimensionalize the temperature is considered as  $W_{f,s} = \frac{\gamma_{f,s} V L}{k_{f,s}}$ . Accordingly, we attempt the solution of the

one-dimensional (1D) form of the equations (4a-4h) given by.

$$-(2 + \lambda_1) \frac{d^2 V_f}{dx^2} + \phi_f \frac{dP}{dx} + \frac{1}{Da} V_f = 0, \quad (15a)$$

$$-(2 + \lambda_2) \frac{d^2 U_s}{dx^2} + \phi_s \frac{dP}{dx} - \frac{1}{Da} V_f + \delta_s \Xi \frac{\partial \theta_s}{\partial x} = 0, \quad (15b)$$

$$\frac{d}{dx} (\phi_f V_f) = a_2 - a_1 P, \quad (15c)$$

$$\text{Pe}_f \left( \frac{\partial}{\partial x} (\theta_f V_f) \right) - \frac{\partial^2 \theta_f}{\partial x^2} = -N(\theta_f - \kappa \theta_s) - \frac{dV_f}{dx}, \quad (15d)$$

$$-\frac{\partial^2 \theta_s}{\partial x^2} = -N(\kappa \theta_s - \theta_f). \quad (15e)$$

Note that the last term on the left of the equation (15b) contains an extra coefficient  $\Xi$ . For  $\Xi = 1$ , the solid displacement depends on the thermal variation due to the hydrodynamic inside the medium. Whereas, for  $\Xi = 0$ , the solid displacement is not influenced by the solid displacement and one may obtain the corresponding analytical exact solution.

### Boundary conditions

The fluid velocity at the inlet is considered to be the same as the characteristic fluid velocity and at the outlet, fluid flux is assumed to be zero. Accordingly, the boundary conditions for the fluid velocity is given by

$$V_f = 1, \quad \text{at } x = 0; \quad (16a)$$

$$\frac{dV_f}{dx} = 0, \quad \text{at } x = 1. \quad (16b)$$

For the solid displacement, we consider the solid structure to be fixed at both ends as

$$U_s = 0, \quad \text{at } x = 0; \quad (17a)$$

$$U_s = 0, \quad \text{at } x = 1. \quad (17b)$$

A fixed temperature is maintained at the inlet of the domain  $\Omega$  and the temperature flux is considered to be zero at the outlet, accordingly, the thermal boundary conditions are given by

$$\theta_s = 1 \quad \text{at } x = 0, \quad (18a)$$

$$\theta_f = 1 \quad \text{at } x = 0, \quad (18b)$$

$$\frac{d\theta_s}{dx} = 0 \quad \text{at } x = 1, \quad (18c)$$

$$\frac{d\theta_f}{dx} = 0 \quad \text{at } x = 1. \quad (18d)$$

Using the steady thermoelastic balance (15d-15e), we get the fourth-order differential equation as

$$\frac{d^4 \theta_s}{dx^4} - \text{Pe}_f V_f \frac{d^3 \theta_s}{dx^3} + \left( (\kappa + 1)N - \text{Pe}_f \frac{dV_f}{dx} \right) \frac{d^2 \theta_s}{dx^2} - \text{Pe}_f N \kappa V_f \frac{d\theta_s}{dx} - \text{Pe}_f \kappa N \frac{dV_f}{dx} \theta_s = N \frac{dV_f}{dx}. \quad (19)$$

The corresponding boundary conditions (18a-18d) are given by

$$\theta_s = 1 \quad \text{at } x = 0, \quad (20a)$$

$$\kappa \theta_s + \frac{1}{N} \frac{d^2 \theta_s}{dx^2} = 1 \quad \text{at } x = 0, \quad (20b)$$

$$\frac{d\theta_s}{dx} = 0 \quad \text{at } x = 1, \quad (20c)$$

$$\kappa \frac{d\theta_s}{dx} + \frac{1}{N} \frac{d^3 \theta_s}{dx^3} = 0 \quad \text{at } x = 1. \quad (20d)$$

## 4.1 Solution procedure

The elasto-hydrodynamic equations (15a and 15c) admit the following general solutions for the fluid velocity and the hydraulic pressure.

$$v_f = Ae^{\alpha_f x} + Be^{-\alpha_f x}, \quad (21a)$$

$$P = \frac{1}{a_2}(a_1 - \phi_f \alpha_f (Ae^{\alpha_f x} + Be^{-\alpha_f x})), \quad (21b)$$

where  $a_1 = \frac{a_0 L P_a}{V}$ ,  $a_2 = \mu_f a_0$ , and

$$\alpha_f^2 = \frac{1}{Da} \left( 2 + \lambda_1 + \frac{\phi_f^2}{a_2} \right)^{-1}. \quad (22)$$

Using the boundary conditions (16a-16b), the constants  $A$  and  $B$  for the fluid velocity are given by

$$A = 1 - \frac{1}{e^{\alpha_f} - e^{-\alpha_f}}, \quad B = \frac{1}{e^{\alpha_f} - e^{-\alpha_f}}. \quad (23)$$

For the case  $\Xi = 0$ , using (21a) and (21b) the momentum balance for the displacement (equation 15b) admits the general solution as follows

$$u_s = \frac{\alpha_s}{\alpha_f} (Ae^{\alpha_f x} + Be^{-\alpha_f x}) + Cx + D, \quad (24)$$

where

$$\alpha_s = -(2 + \lambda_2)^{-1} \left( \frac{\phi_f \phi_s \alpha_f^2}{a_2} + \frac{1}{Da} \right).$$

The arbitrary constants  $C$  and  $D$  are obtained using the boundary conditions (17a-17b) as follows

$$D = -\frac{\alpha_s}{\alpha_f} * (A + B), \quad (25)$$

$$C = -\frac{\alpha_s}{\alpha_f} (A * e^{\alpha_f} + B * e^{-\alpha_f}) - D. \quad (26)$$

In order to obtain the solution for the case  $\Xi = 1$ , we solve the equation (4) along with the boundary conditions (20a-20d) numerically using the finite difference method. We have used MATLAB R2023a to generate numerical results.

## 5 Results and Discussion

In this section, we present certain significant results displaying the impact of various physical parameters on both elastodynamics and thermodynamics. The parameter values considered to obtain the results are provided in Table 3. Further, among numerous intrinsic relations between the porosity and the permeability, in the case of the tumor, we consider the Carman-Kozeny (CK) equation given by

$$\mu_f K = \frac{\phi_f^3}{C_k (1 - \phi_f)^2 D_c^2},$$

where  $C_k$  is the Carman-Kozeny constant and  $D_c$  is the average cell diameter per unit volume of the tumor [27]. Here, the CK constant takes the value 2 for porosity  $\phi_f \geq 0.9$  and 3 – 5 for porosity  $\phi_f < 0.9$ .

In Figure 2 and 3, we compare the hydrodynamics and elasto-thermodynamics for the high Darcy and low Darcy numbers, respectively. One may observe that the fluid velocity profile is significantly higher for the large Darcy number due to less resistance offered by the porous medium (Figure 2). However, the displacement of the solid phase is minimal in this case due to less contribution of the hydrodynamic pressure. Contrary to this, in the low Darcy number regime, the solid displacement profile is more pronounced due to the force exerted by the fluid

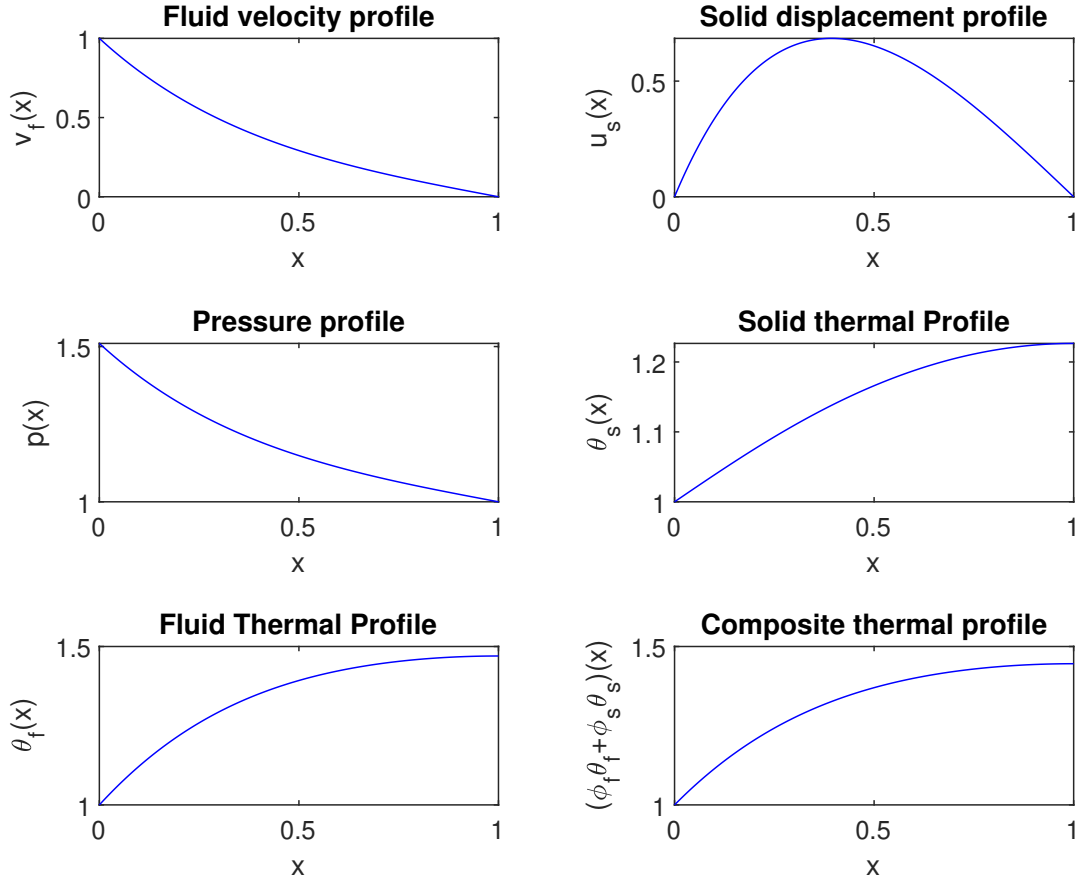


**Figure 2:** For high porosity  $\phi_f = 0.9$ , permeability  $Da = 0.0583$ , and  $\kappa_f = 5$ ,  $\kappa_s = 5$ ,  $N = 2$ ,  $Pe_f = 0.7596$ .

flow. The pressure profile justifies the behavior of solid displacement and fluid velocity in both cases (see Figure 3). Here, we fix the thermal conductivity for the solid and fluid phase at the same value  $\kappa_f = \kappa_s = 5$ . In this scenario, the thermal conduction is dominated by the thermal convection ( $Pe_f = 0.7596$ ) assisted by fluid flow. Moreover, due to the viscous dissipation, the fluid temperature is higher than the inlet temperature throughout the length of the biomass. Consequently, the solid phase temperature is enhanced due to the heat exchange (here,  $h = 10$  dimensional form and nondimensional form  $N = 2$ , see Figure 2). In the low Darcy case, the impact of the convection on the fluid temperature is negligible. As a result, the solid temperature also reduces due to low exchange. One may observe that the composite temperature is dominated by the fluid volume fraction and behaves in accordance.

So far we have witnessed the elastodynamics and thermoelasticity concerning the change in the Darcy medium fixing other parameters such as thermal conductivity and heat exchange coefficient. In Figure 4, we analyze the thermal profile reducing the heat exchange rate to  $N = 0.2$  and keeping the heat diffusivity of the fluid and solid medium as  $\kappa_f = 5 = \kappa_s$ . In the highly permeable biomass, convection dominates dissipation and assists the fluid temperature. Convection of the fluid phase depends on the specific heat capacity  $c_f$ , which is the amount of heat energy the fluid can carry per unit mass. Accordingly, this becomes responsible for the rise in the fluid temperature along the length. However, due to the low exchange rate of heat, the solid temperature decreases along the length. Overall, one may observe a rise in the composite temperature due to the low exchange rate. Note that the difference in the thermal heat conductivity of the fluid and solid phases may induce varied patterns as explained in the next figure.

Figure 5 corresponds to unequal diffusivity of the solid and fluid phases with  $\kappa_f = 5$  and  $\kappa_s = 1$  so that a high thermal conductivity ratio ( $\kappa = \kappa_f/\kappa_s$ ) persists. This leads to decreasing solid temperature due to a low exchange

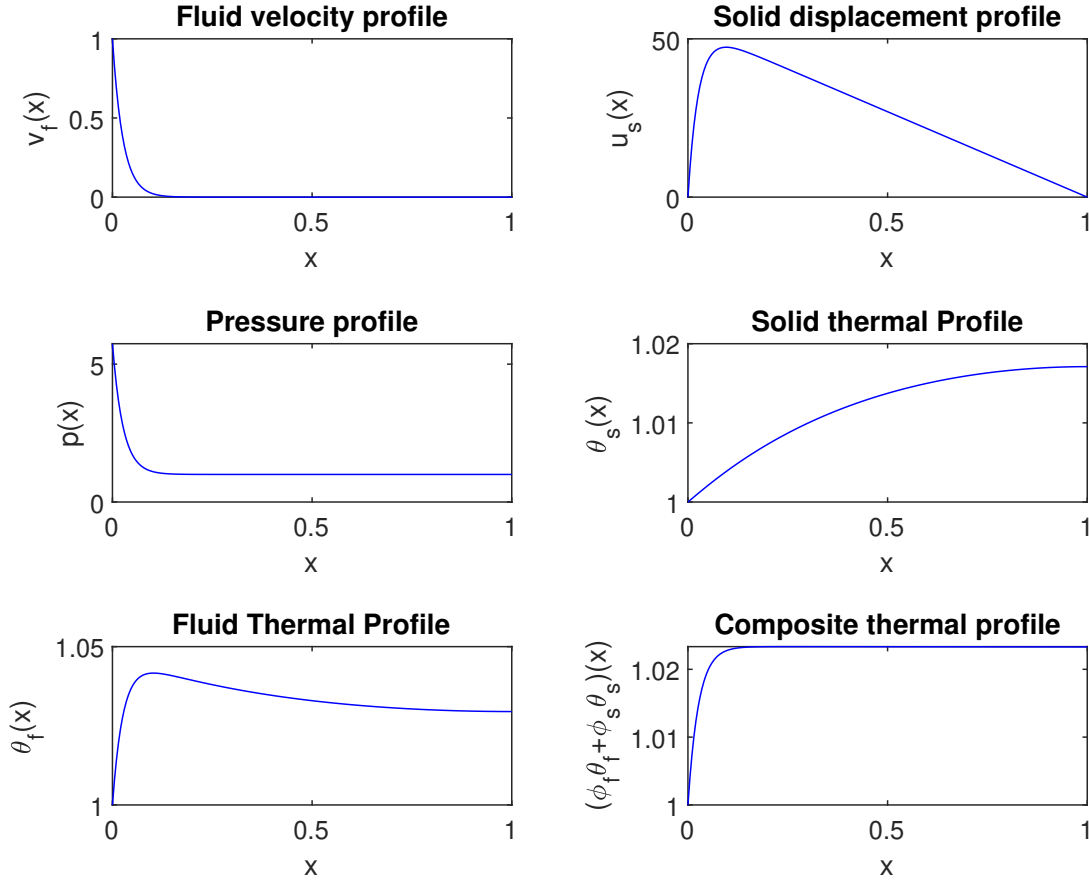


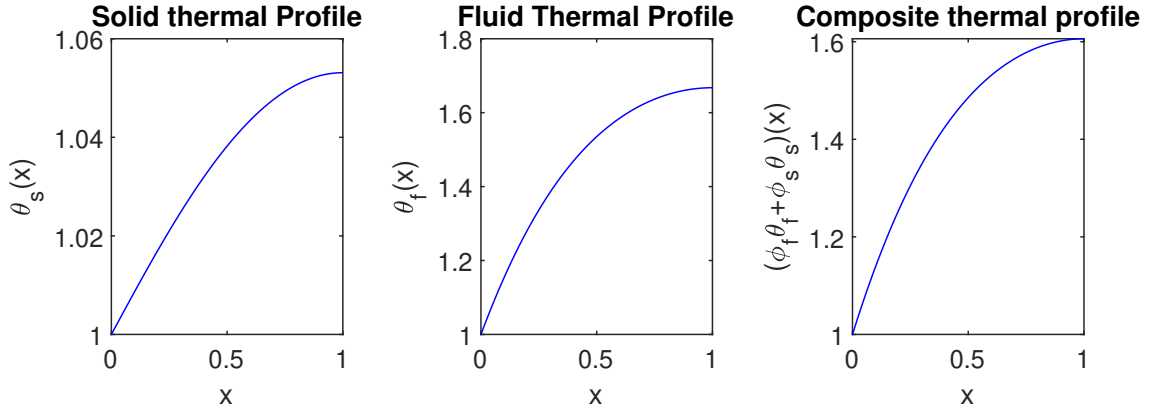
**Figure 3:** For low porosity  $\phi_f = 0.5$  permeability,  $Da = 0.0002$ , and  $\kappa_f = 5$ ,  $\kappa_s = 5$ ,  $N = 2$ ,  $Pe_f = 0.7596$ .

rate,  $N = 0.2$ . The temperature within the fluid phase is assisted by the convection as well as conductivity which keeps the inlet temperature high. Consequently, the composite thermal profile increases primarily driven by the higher fluid temperature and significant volume fraction  $\phi_f = 0.9$ . In contrast, when  $\kappa_f = 1$  and  $\kappa_s = 5$ , both the solid and fluid temperatures increase (see Figure 5). Here, the exchange rate is higher, with  $N = 1$ , and the Peclet number is  $Pe_f = 3.7978$ . As a result, the fluid temperature is higher than that of the previous case (as shown in Figure 6). The composite thermal profile also increases influenced by the elevated fluid temperature dominated by its volume fraction and supported by the increasing solid temperature.

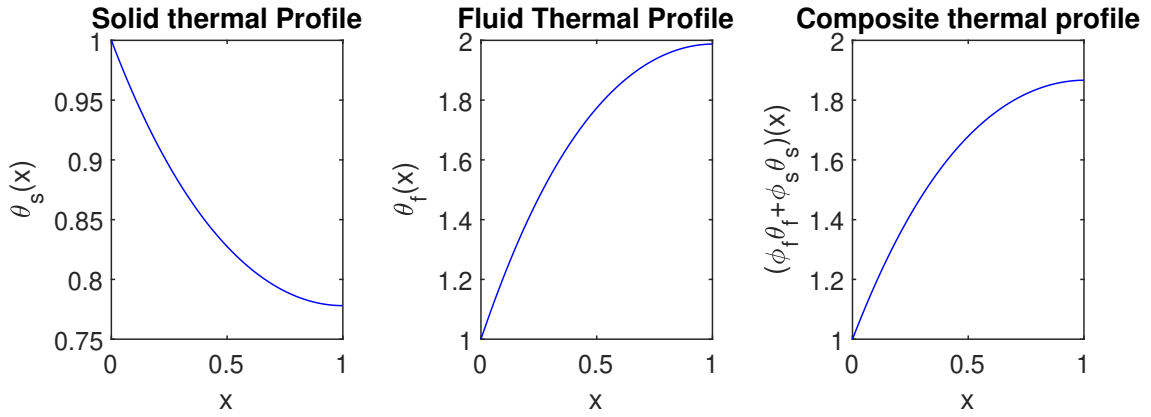
Figure 7(a) represents the solid and fluid thermal profiles while the conductivity of the liquid phase is fixed at  $\kappa_f = 5$  and the solid phase heat conductivity is varied. Under this scenario, the thermal exchange parameter and the Peclet number remain constant as  $N = 0.2$  and  $Pe_f = 0.7596$ . Although the exchange parameter remains constant the conductivity ratio  $\kappa$  increases reducing the solid thermal conductivity  $\kappa_s$ . This reduces the solid temperature with declining solid thermal conductivity whereas the fluid temperature increases due to the interaction force. In Figure 7(b), the solid thermal conductivity is fixed at  $\kappa_s = 5$  while the fluid thermal conductivity is varied. Here we observe that the Peclet number depends inversely on the liquid thermal conductivity. As a result, we witness a drop in the fluid temperature with increasing thermal conductivity. It is to be noticed that the heat exchange parameter  $N$  is decreasing with increasing fluid thermal conductivity, however, due to increasing conductivity ratio  $\kappa$  the overall domination of heat exchange results in decreasing solid thermal profile.

Figure 8(a) displays the solid displacement profiles for  $\Xi = 0$  and  $\Xi = 1$  when the porosity of the biomass is considered to be  $\phi^f = 0.8$  and the permeability at  $Da = 0.0583$ . Here, the Peclet number and the heat exchange parameters remain constant for fixed fluid conductivity  $\kappa_f = 5$ . While  $\Xi = 1$ , the ratio of thermal expansion to the viscous forces  $\delta_s$  is effective and decreases with increasing solid thermal conductivity. Moreover, we





**Figure 4:** For high porosity  $\phi_f = 0.9$ , permeability  $Da = 0.0583$ , and  $\kappa_f = 5$ ,  $\kappa_s = 5$ ,  $N = 0.2$ ,  $Pe_f = 0.7596$ .



**Figure 5:** For high porosity  $\phi_f = 0.9$ , permeability  $Da = 0.0583$ , and  $\kappa_f = 5$ ,  $\kappa_s = 1$ ,  $N = 0.2$ ,  $Pe_f = 0.7596$ .

witnessed earlier that the solid temperature decreases with decreasing solid thermal conductivity. Consequently, we observe that the difference between the solid displacement when the thermal expansion is effective  $\Xi = 1$  and ineffective  $\Xi = 0$  is reduced, and the solid thermal conductivity increases. This resembles the impact of thermal expansion related to  $\delta_s$  onto the solid temperature. When the thermal conductivities of fluid and solid are equal at  $\kappa_f = \kappa_s = 5$  and the thermal expansion parameter  $\alpha_s$  is reduced, we observe the reduced difference in solid displacement profile pertaining to  $\Xi = 0$  and  $\Xi = 1$  (see Figure 8(b)). Note that  $\delta_s$  decreases while the thermal expansion parameter  $\alpha_s$  decreases.

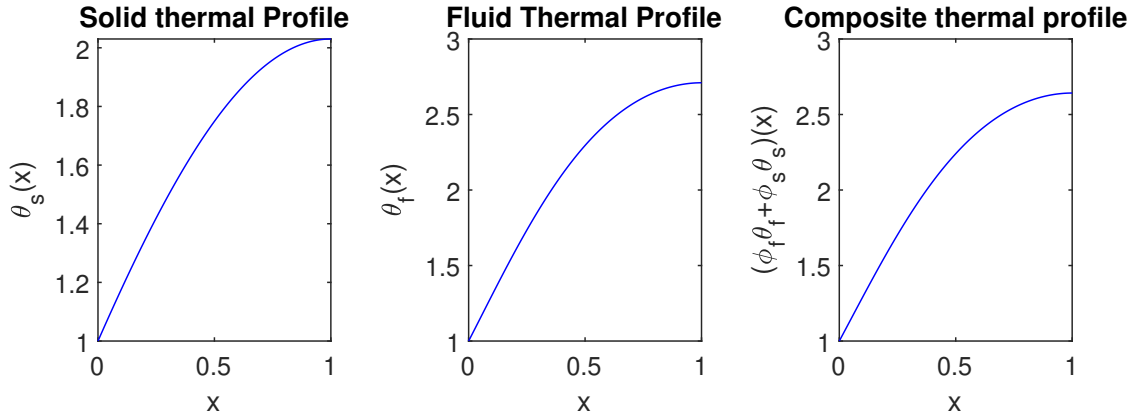


Figure 6: For high porosity  $\phi_f = 0.9$ , permeability  $Da = 0.0583$ , and  $\kappa_f = 1$ ,  $\kappa_s = 5$ ,  $N = 1$ ,  $Pe_f = 3.7978$ .

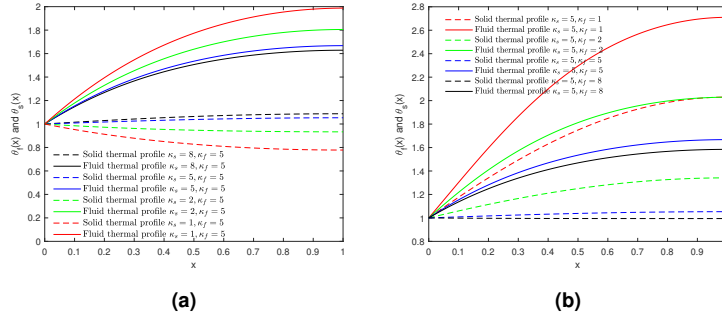
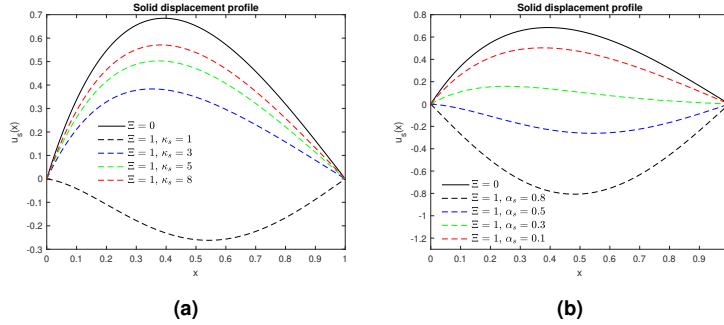


Figure 7: Thermal profiles of solid and fluid phases. (a) For fixed thermal conductivity  $\kappa_f = 5$  and varying  $\kappa_s$  when the thermal exchange coefficients  $N = 0.2$  and  $Pe_f = 0.7596$ . (b) For fixed thermal conductivity  $\kappa_s = 5$  and varying  $\kappa_f$  where the thermal exchange coefficient and Peclet number depends on  $\kappa_f$ .

Variable	Value	Unit	Description
$\rho_s$	1100	kg/m <sup>3</sup>	Mass density (solid)
$\rho_f$	1050	kg/m <sup>3</sup>	Mass density (fluid)
$c_s$	2500	J/(kg * K)	Specific heat (solid)
$c_f$	3617	J/(kg * K)	Specific heat (fluid)
$k_s$	5	W/(m * K)	Heat conductivity (solid)
$k_f$	5	W/(m * K)	Heat conductivity (fluid)
$\alpha$	10	W/(m <sup>3</sup> *K)	Heat exchange coefficient
$\mu_s$	2	MPa	Viscosity (solid)
$\mu_f$	0.0026	Pa * s	Viscosity (fluid)
$\lambda_s$	.8	MPa	Lame (solid)
$\lambda_f$	0.004	Pa * s	Lame (fluid)
$\gamma_s$	0.5	W * s/m <sup>3</sup>	Thermal expansion (solid)
$\gamma_f$	0.5	W * s/m <sup>3</sup>	Thermal expansion (fluid)
$K$	1	m <sup>2</sup>	Drag coefficient
$\beta$	0.001		Pressure coefficient
$\varphi_s$	.7		Volume fraction (solid)
$\varphi_f$	.3		Volume fraction (fluid)

Table 3: Possible set of parameter and coefficient choices for the simulations.



**Figure 8:** Solid displacement profile when thermal expansion is effective  $\Xi = 1$  and non-effective  $\Xi = 0$ . (a) The thermal conductivity of a solid is  $\kappa_s = 1, 3, 5, 8$  while the thermal conductivity of fluid is fixed as  $\kappa_f = 5$ . (b) The thermal expansion of the solid phase is  $\alpha_s = 0.1, 0.3, 0.5, \text{ and } 0.8$ .

## 6 Conclusions

We proposed and investigated an intricately coupled model where hydrodynamic poroelasticity interacts in interesting ways with the heat transfer in the system. Making use of the well-established theory of implicit evolution equations together with a careful analysis of the time regularity of the solutions to the hydrodynamic subproblem, we established well posedness of this model. We then took a simplified radially symmetric setup of our problem to further highlight the coupling mechanism by semi-analytical solutions and numerical solutions to the problem.

We want to point out that the coupling in our model and the corresponding analysis is able to account for non-constant coefficients as well as some *well behaved* non-linearities without much effort. As one example, via a standard fixed-point argument utilizing the contraction mapping principle it is possible to include temperature effects in the viscosity, i.e.,  $\lambda_1 = \lambda_1(\theta_f)$  for  $\lambda_1: \mathbb{R} \rightarrow \mathbb{R}$  bounded and Lipschitz continuous.

We have analyzed the system using a simplified 1D Cartesian coordinate framework considering a sufficiently small timescale approach. We observed, that the heat dissipation has a significant impact on the fluid and solid thermal profiles. The fluid thermal profile is supported by convection as well as dissipation, whereas the solid thermal profile follows the interaction with the fluid temperature. In future work, we plan to include actual mechanics of tumor growth.

## Conflict of interest

On behalf of all authors, the corresponding author states that there is no conflict of interest.

## Data availability statement

Data will be made available on request.

## References

- [1] M. Alam, H. Byrne, and G. Raja Sekhar. Existence and uniqueness results on biphasic mixture model for an in-vivo tumor. *Applicable Analysis*, 101(15):5442–5468, 2022.
- [2] M. Alam, B. Dey, and G. R. Sekhar. Mathematical modeling and analysis of hydroelastodynamics inside a solid tumor containing deformable tissue. *ZAMM-Journal of Applied Mathematics and Mechanics/Zeitschrift für Angewandte Mathematik und Mechanik*, 99(5):e201800223, 2019.
- [3] D. Ambrosi and L. Preziosi. On the closure of mass balance models for tumor growth. *Math. Models Methods Appl. Sci.*, 12(5):737–754, 2002.

- [4] A. Andreozzi, M. Iasiello, and P. A. Netti. A thermoporoelastic model for fluid transport in tumour tissues. *J. R. Soc. Interface*, 16(154):20190030, May 2019.
- [5] S. Astanin and L. Preziosi. Multiphase models of tumour growth. In *Selected topics in cancer modeling: Genesis, evolution, immune competition, and therapy*, pages 1–31. Springer, 2008.
- [6] G. A. Ateshian. On the theory of reactive mixtures for modeling biological growth. *Biomechanics and Modeling in Mechanobiology*, 6(6):423–445, Jan. 2007.
- [7] M. M. Attar, M. Haghpanahi, H. Shahverdi, and A. Imam. Thermo-mechanical analysis of soft tissue in local hyperthermia treatment. *J. Mech. Sci. Technol.*, 30(3):1459–1469, Mar. 2016.
- [8] L. T. Baxter and R. K. Jain. Transport of fluid and macromolecules in tumors. i. role of interstitial pressure and convection. *Microvascular Research*, 37(1):77–104, 1989.
- [9] R. M. Bowen. Part i - theory of mixtures. In A. C. ERINGEN, editor, *Continuum Physics*, pages 1–127. Academic Press, 1976.
- [10] H. Byrne and L. Preziosi. Modelling solid tumour growth using the theory of mixtures. *Mathematical medicine and biology : a journal of the IMA*, 20 4:341–66, 2003.
- [11] R. T. C. Truesdell. The classical field theories, in: Handboub der physik vol. iii/3. *Handboub der Physik*, 1960.
- [12] O. Coussy. *Poromechanics*. John Wiley & Sons, 2004.
- [13] B. Dey and G. P. R. Sekhar. Hydrodynamics and convection enhanced macromolecular fluid transport in soft biological tissues: Application to solid tumor. *Journal of Theoretical Biology*, 395:62–86, 2016.
- [14] B. Dey, G. P. R. Sekhar, and S. K. Mukhopadhyay. In vivo mimicking model for solid tumor towards hydromechanics of tissue deformation and creation of necrosis. *Journal of Biological Physics*, 44(3):361–400, May 2018.
- [15] F. Dobran. Theory of multiphase mixtures—a thermomechanical formulation. *International Journal of Multiphase Flow*, 11(1):1–30, 1985.
- [16] G. Duvaut and J. L. Lions. *Inequalities in Mechanics and Physics*. Springer Berlin Heidelberg, 1976.
- [17] M. Eden and A. Muntean. Homogenization of a fully coupled thermoelasticity problem for a highly heterogeneous medium with *a priori* known phase transformations. *Math. Methods Appl. Sci.*, 40(11):3955–3972, 2017.
- [18] A. C. Eringen and J. D. Ingram. A continuum theory of chemically reacting media—i. *International Journal of Engineering Science*, 3(2):197–212, 1965.
- [19] L. Evans. *Partial Differential Equations*. American Mathematical Society, Mar. 2010.
- [20] J. R. Fernández and M. Masid. A mixture of thermoelastic solids with two temperatures. *Computers & Mathematics with Applications*, 73(9):1886–1899, 2017.
- [21] C. Giverso, M. Scianna, and A. Grillo. Growing avascular tumours as elasto-plastic bodies by the theory of evolving natural configurations. *Mechanics Research Communications*, 68:31–39, Sept. 2015.
- [22] A. Green and P. Naghdi. A dynamical theory of interacting continua. *International Journal of Engineering Science*, 3(2):231–241, 1965.
- [23] A. Green and P. Naghdi. A note on mixtures. *International Journal of Engineering Science*, 6(11):631–635, 1968.
- [24] D. Ieşan. On the theory of mixtures of thermoelastic solids. *Journal of Thermal Stresses*, 14(4):389–408, 1991.

- [25] J. D. Ingram and A. Cemal Eringen. A continuum theory of chemically reacting media—ii constitutive equations of reacting fluid mixtures. *International Journal of Engineering Science*, 5(4):289–322, 1967.
- [26] V. D. Kupradze. *Three-dimensional problems of the mathematical theory of elasticity and thermoelasticity*. North-Holland Pub. Co. Sole distributors for the U.S.A. and Canada Elsevier/North-Holland, Amsterdam New York New York, 1979.
- [27] S. Majumder, M. T. Islam, and R. Righetti. Non-invasive imaging of interstitial fluid transport parameters in solid tumors in vivo. *Scientific Reports*, 13(1):7132, 2023.
- [28] P. A. Netti, L. T. Baxter, Y. Boucher, R. Skalak, and R. K. Jain. Macro- and microscopic fluid transport in living tissues: Application to solid tumors. *AIChE Journal*, 43(3):818–834, 1997.
- [29] C. S. Park, C. Liu, S. K. Hall, and S. J. Payne. A thermoelastic deformation model of tissue contraction during thermal ablation. *Int. J. Hyperthermia*, 34(3):221–228, Apr. 2018.
- [30] L. Preziosi. The theory of deformable porous media and its application to composite material manufacturing. *Surveys Math. Indust.*, 6(3):167–214, 1996.
- [31] L. Preziosi and A. Tosin. Multiphase modelling of tumour growth and extracellular matrix interaction: mathematical tools and applications. *Journal of mathematical biology*, 58:625–656, 2009.
- [32] K. R. Rajagopal and L. Tao. *Mechanics of mixtures*, volume 35 of *Series on Advances in Mathematics for Applied Sciences*. World Scientific Publishing Co., Inc., River Edge, NJ, 1995.
- [33] R. Showalter. *Monotone Operators in Banach Space and Nonlinear Partial Differential Equations (Mathematical Surveys and Monographs)*. American Mathematical Society, 12 1996.
- [34] R. Showalter and B. Momken. Single-phase flow in composite poro-elastic media. *Mathematical Methods in the Applied Sciences*, 25:115–139, 2002.
- [35] J. Simon. Compact sets in the space  $L^p(0, T; B)$ . *Annali di Matematica Pura ed Applicata*, 146(1):65–96, Dec. 1986.
- [36] M. S. T. Burchuladze. Potential method in the linear theory of binary mixtures of thermoelastic solids. *Journal of Thermal Stresses*, 23(6):601–626, 2000.
- [37] C. Truesdell. *Rational Thermodynamics*. Springer New York, 1984.
- [38] Y. Z. Wang, M. J. Li, and D. Liu. Thermo-mechanical interaction on transient heating of skin tissue with variable thermal material properties. *Eur. J. Mech. A Solids*, 86(104173):104173, Mar. 2021.
- [39] P. Yuan, H.-E. Liu, C.-W. Chen, and H.-S. Kou. Temperature response in biological tissue by alternating heating and cooling modalities with sinusoidal temperature oscillation on the skin. *International Communications in Heat and Mass Transfer*, 35(9):1091–1096, Nov. 2008.
- [40] J. Zhang, R. J. Lay, S. K. Roberts, and S. Chauhan. Towards real-time finite-strain anisotropic thermo-visco-elastodynamic analysis of soft tissues for thermal ablative therapy. *Computer Methods and Programs in Biomedicine*, 198:105789, Jan. 2021.